JACS
JOURNAL OF THE AMERICAN CHEMICAL SOCIETY
Article
pubs.acs.org/JACS

Coupling of Carbon and Peptide Nanotubes

Javier Montenegro,*[,†] Carlos Vázquez-Vázquez,[‡] Arseny Kalinin,[§] Kurt E. Geckeler,[∥] and Juan R. Granja*[,†]

[†]Singular Research Centre in Chemical Biology and Molecular Materials (CIQUS), Organic Chemistry Department, University of Santiago de Compostela (USC), Santiago de Compostela 15782, Spain

[‡]Technological Research Institute (IIT), Physical Chemistry Department, University of Santiago de Compostela (USC), Santiago de Compostela 15782, Spain

[§]NT-MDT and Moscow Institute of Physics and Technology (MIPT), Moscow 117810, Russia

[∥]Department of Materials Science and Engineering Gwangju Institute of Science & Technology, Oryong-dong, Buk-gu, Gwangju 500-712, South Korea

Supporting Information

ABSTRACT: Two of the main types of nanotubular architectures are the single-walled carbon nanotubes (SWCNTs) and the self-assembling cyclic peptide nanotubes (SCPNs). We here report the preparation of the dual composite resulting from the ordered combination of both tubular motifs. In the resulting architecture, the SWCNTs can act as templates for the assembly of SCPNs that engage the carbon nanotubes noncovalently via pyrene "paddles", each member of the resulting hybrid stabilizing the other in aqueous solution. The particular hybrids obtained in the present study formed highly ordered oriented arrays and display complementary properties such as electrical conductivity. Furthermore, a self-sorting of the cyclic peptides toward semiconducting rather than metallic SWCNTs is also observed in the aqueous dispersions. It is envisaged that a broad range of exploitable properties may be achieved and/or controlled by varying the cyclic peptide components of similar SWCNT/SCPN hybrids.

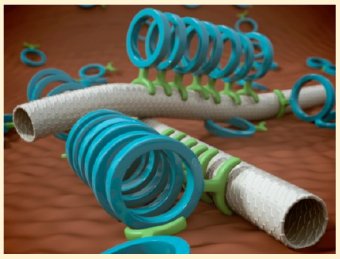

INTRODUCTION

Hollow nanometric structures play diverse important roles in biology, nanotechnology, and materials science.[1] Examples include viral capsids, certain enzymes, ion channels, and the pores of ultrafine separation systems. Two of the main types of synthetic tubular nanometric structures are the single-wall carbon nanotubes (SWCNTs) and the self-assembled cyclic peptide nanotubes (SCPNs), which have similar dimensional features but different and complementary properties. Individual SWCNTs have extraordinary mechanical and electronic properties that depend on their diameter and chirality.[2] However, the remarkable properties of carbon nanotubes (CNTs) are intrinsically limited by their synthetic and structural boundaries, together with their low solubility and self-aggregation propensity. The prospective challenges for SWCNTs applications have boosted the creativity of worldwide researchers prompting many elegant approaches to exploit this novel nanomaterial.[3−14] In addition to covalent chemistry,[6,7] noncovalent modification[8] have arisen as a powerful strategy for SWCNT manipulation because they are reversible and they preserve the CNT structural integrity. Nevertheless, it is also feasible to fine-tune the properties of SWCNTs by using supramolecular approaches.[8−10] SWCNTs are prepared as polydisperse mixtures, while many of the most ambitious proposals for their technological application require, or would be best implemented by, ordered arrays of CNTs with uniform characteristics.[11] For example, CNT-based field effect transistors would ideally employ ordered arrays of exclusively semiconducting SWCNTs.[11b] Along these lines, current techniques for separating different CNTs species can benefit from their solubilization with surfactants, dyes, or DNA.[12−14]

SCPNs are supramolecular polymers formed by the stacking of appropriate cyclic peptides (CPs) via hydrogen bonds. Suitable CPs with alternating chirality in their amino acid sequence adopt a planar conformation in which the amino acid side chains radiate outward from the peptide ring while the amide carbonyl and NH groups are oriented perpendicular to the peptide plane, allowing the formation of hydrogen bond networks. The straightforward synthesis of CPs, with complete control over CP ring diameter and side chain functionalization, are major advantages of these kind of nanotubes, which find applications ranging from ion separation to electroactive molecule templation and antimicrobial therapy.[1,15−17]

The nanometric topological control of supramolecular ensembles of carbon nanotubes and the possible alignment of molecules of interest along the longitudinal axis of carbon nanotubes are major challenges for the development of novel hybrids with adjusted and improved properties. Along these lines, the preparation of carbon and peptide dual tubular materials might benefit from the particular different and complementary properties of both molecular entities. For example, in electrical responsive sensors, the cyclic peptide ring might help in the alignment of any desired recognition moiety

Received: October 24, 2013
Published: January 16, 2014

   dx.doi.org/10.1021/ja410901r | J. Am. Chem. Soc. 2014, 136, 2484−2491

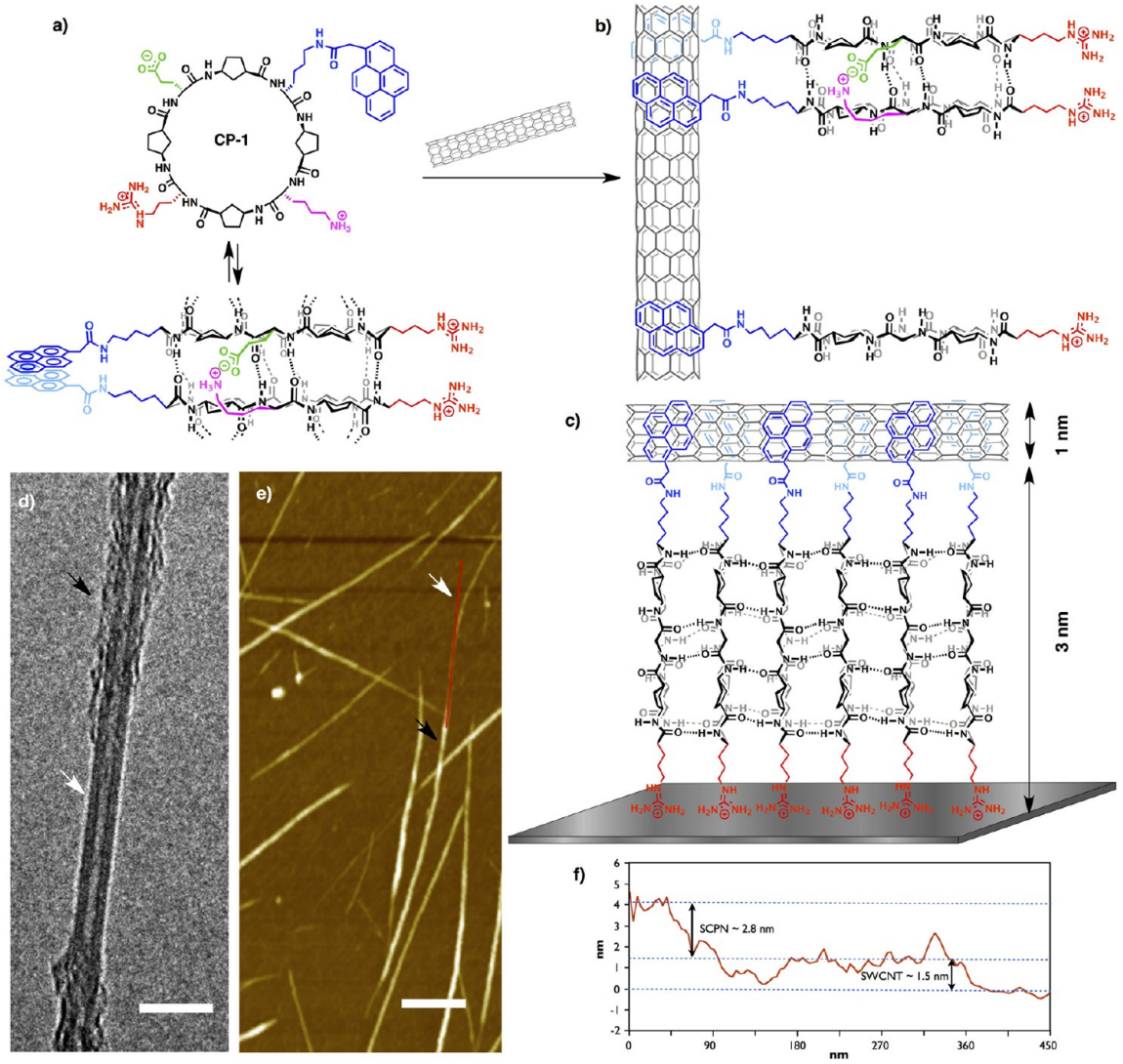

Figure 1. Proposed model of coupling between SCPNs and SWCNTs, and representative TEM and AFM images. (a) Structures of **CP-1** and of a dimer that represents the minimal supramolecular entity of the corresponding SCPN. (b) Plausible model of the coupling of **CP-1** to CNTs, which is hypothesized as favoring the orderly association of **CP-1** units in SCPNs. (c) Plausible model of the attachment of SWCNT/SCPN hybrids to an anionic surface. (d) TEM image of a SWCNT/SCPN hybrids after deposition from dispersion on a carbon holey grid. The white arrow indicates an SCPN-free segment of CNT, the black arrow a hybridized segment (scale bar 5 nm). (e) AFM topographic image of dialyzed aqueous dispersions of SWCNT/SCPN hybrids deposited on mica (grade V-1 muscovite, scale bar 200 nm), arrows as in (d). (f) AFM height profile along the longitudinal axis of a nanotube (red line).

incorporated in the peptide sequence. We could even envisage the preparation of optimized ion channel templates or even donor–acceptor energy devices. Furthermore, biomedical applications of dual peptide/carbon nanotubes might benefit from peptide biocompatibility, influencing not only the solubilization of the carbon tube in biological media, but also rendering novel and improved properties of the resulting amphiphilic dynamic structure.

In this work, we report preparative synergies between SWCNTs and SCPNs. More specifically, we have designed CPs that engage CNTs noncovalently and thereby exploit them as a rigs for the assembly of the CPs into SCPNs. Attachment to the π surface of CNTs stabilizes the assembly of peptide nanotubes, and the hydrophilic side chains on the attached SCPNs in turn stabilize the CNTs in aqueous solution. This parallel "*dual-tube*" disposition should allow for the alignment (along the CNT) of molecules of interest that would be attached to the cyclic peptide ring or even facilitate possible double flow transport of different ions or molecules through the cavity of each nanotube.[15,18] The SWCNT/SCPN hybrids obtained in this work also formed highly ordered oriented arrays when deposited on glass or mica. Furthermore, the general strategy described here for their preparation will allow future exploration of dual tubular hybrids with specific features adjusted for particular functions.

RESULTS

Design. With a view to engagement of CNTs, solubility in water, biocompatibility, and stability under physiological conditions, the CP employed was the amphiphilic α,γ-cyclic octapeptide cyclo-[(D-Arg-L-γ-Acp-D-Glu-L-γ-Acp-D-Lys(Pyr)-L-γ-Acp-D-Lys-)] (**CP-1**, Figure 1a). In this CP, 3-aminocyclopentanecarboxylic acid (γ-Acp)[16b] alternates with four α-residues. For engagement of CNTs through water-enhanced π–π interactions[19−23] (Figure 1b), one is a lysine residue

dx.doi.org/10.1021/ja410901r | J. Am. Chem. Soc. 2014, 136, 2484−2491

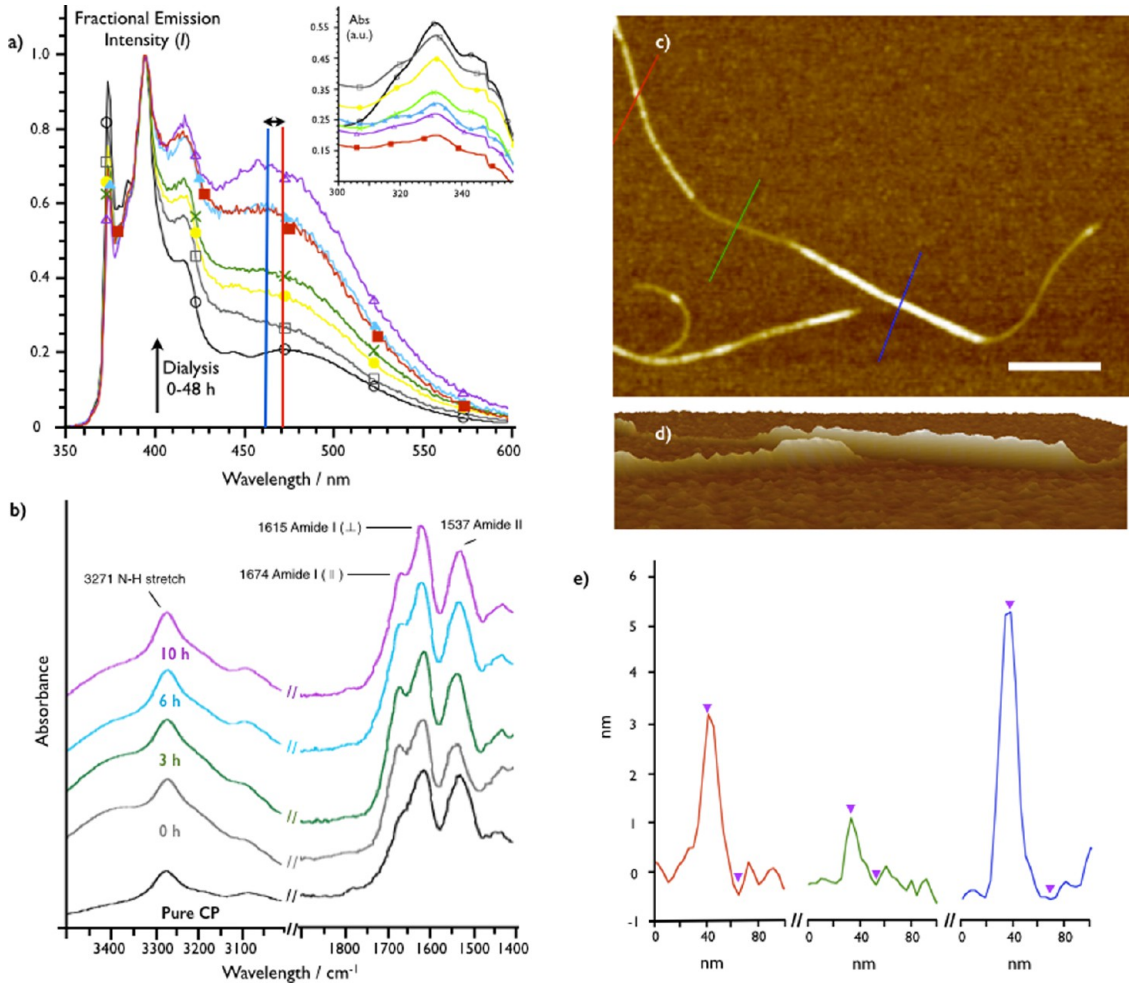

Figure 2. Vis-UV, fluorescence emission and ATR-FTIR spectra, and AFM images and profiles, of SWCNT/SCPN hybrids. (a) Normalized fluorescence emission spectra (λ_{exc} = 340 nm) of 200 μM **CP-1** solution (○) and of SWCNT/SCPN dispersions dialyzed for 0 h (□), 1 h (●), 3 h (×), 6 h (▲), 12 h (△), and 48 h (■). Note the increase and blue shift (by ∼8 nm) of the band around 470 nm due to pyrene exciplex. The inset shows a detail of the Vis-UV absorption spectra of samples diluted 10-fold with respect to those of the main figure. (b) ATR-FTIR spectra of the same solutions and dispersions as in the main figure of (a). (c) AFM topographic image and (d) 3D profile of a CNT coupled for part of its length to an SCPN (scale bar 200 nm). (e) AFM height profiles along the transects shown in (c) through a SWCNT/SCPN segment ∼3.33 nm height (red), an unhybridized CNT segment ∼1.26 nm height (green), and an SCPN/SWCNT/SCPN segment ∼5.74 nm height (blue).

bearing a pyrene "paddle". Opposite this, an arginine favors both solubility in water and adhesion to an anionic hydrophilic surface such as mica (Figure 1c). Between the Arg and Lys(Pyr) residues, a glutamate on one side and a lysine on the other facilitate the stacking of antiparallel oriented CPs through the formation of salt bridges. Such organization favors the formation of the pyrene excimer in solution (Figure 1a) and also would facilitate that the pyrene residues of each CP alternatively wrap one of the faces of the carbon nanotube cylinder (Figure 1b). It was envisaged that once the CPs were attached to the CNT rig, their correct approximation and stacking would be easier than in solution, and that the CNT-CP interaction would lower the concomitant entropic barrier. The viability of the suggested binding model was confirmed, at the molecular level, by minimizing the proposed supramolecular structure by molecular mechanics simulation (Supporting Information, SI, Figure S15).

Preparation and Characterization. **CP-1** was obtained by Fmoc solid phase chemistry[16] on trityl resin, with glutamate as the starting amino acid. After on solid support cyclization, the peptide was cleaved from the resin with trifluoroacetic acid, purified by RP-HPLC, and characterized by ^{1}H NMR, fluorescence and FTIR spectroscopy and atomic force microscopy (AFM). After HPLC purification the overall yield of the synthesis of cyclic peptide was 23%. IR spectra showed intense bands at 1615 and 1537 cm^{-1} identified as amide I and amide II, respectively, corresponding to amide bonds involved in hydrogen bonded antiparallel β-sheets (Figure 2b, bottom trace). The amide A N−H stretching band at 3271 cm^{-1}, confirmed the tight ring-to-ring stacked tubular structure[24] with an average intersubunit distance of 4.70−4.75 Å. Vis-UV fluorescence spectra of aqueous solutions (Figure 2a (○)) showed the typical features of the pyrene chromophore, and the pyrene excimer band at ∼470 nm confirmed the association of CP monomers in solution. The concentration dependence of this band implies an association constant of around 10^3 M^{-1} for nanotube formation at pH 6. The putative tubular supra-structure was confirmed by AFM after deposition on mica of aqueous solutions of **CP-1** followed by rinsing with water. The AFM images showed horizontal fibrous structures with lengths of a few μm and diameters of 2.5−3.0 nm that are in keeping

dx.doi.org/10.1021/ja410901r | J. Am. Chem. Soc. 2014, 136, 2484−2491

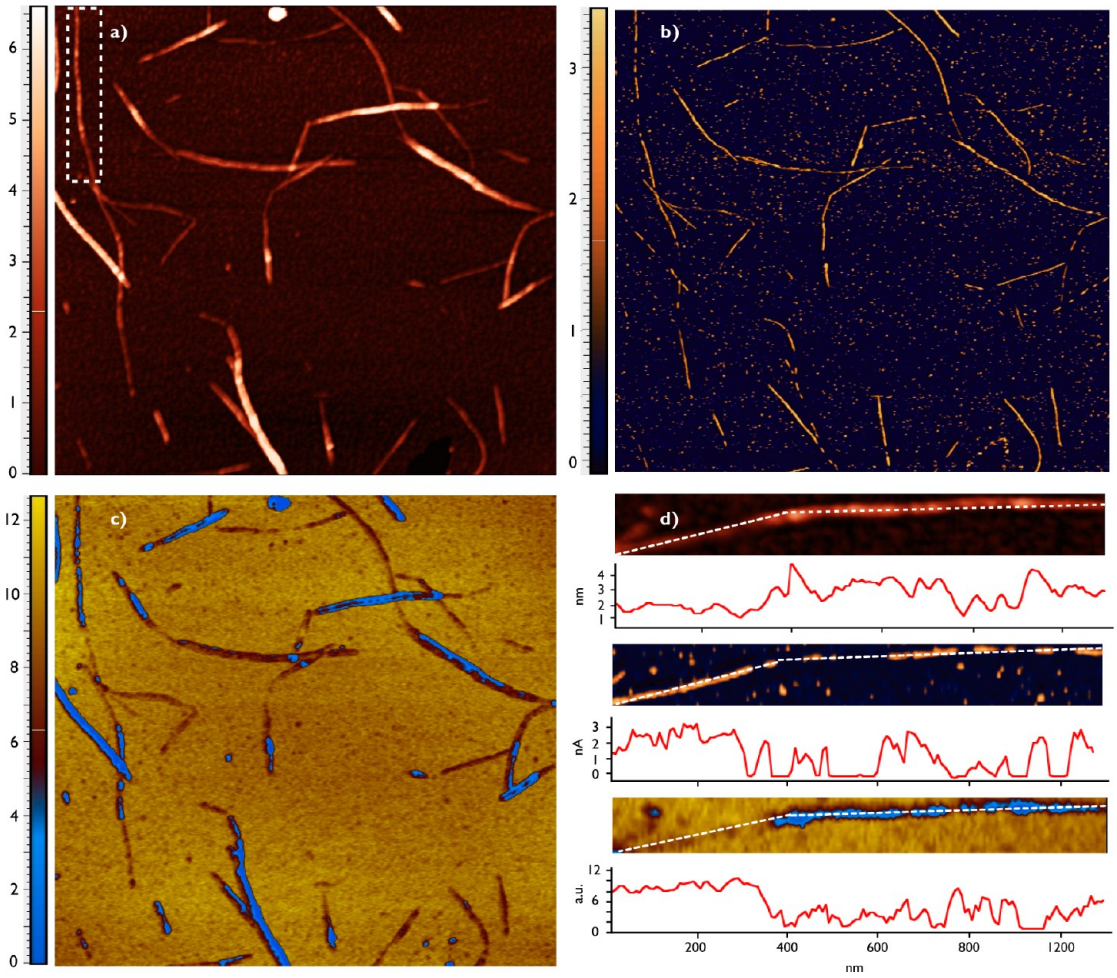

Figure 3. AFM HybriD mode mapping of SWCNT/SCPN hybrids showing topography (a), conductivity (b), elasticity (c), and profiles along the highlighted dual-tube (d). (a) Topography image of a hybrid dispersion showing nanotubes with average diameters between ~4−6 nm and SWCNTs of ~1 nm that increased to 4 and 6 nm (scale bar in nm). (b) Current mapping showing reduction of conductivity up to zero level in high height segments (scale bar in nA, bias potential applied between tip and sample was 1.5 V). (c) Elasticity mapping showing the differences in tubular material elasticity (scale bar in a.u. can be calibrated in Pa, all images are 3.5 × 3.5 μm^2) (the vertical scale bars are in nm, nA and a.u., respectively). (d) Profiles along the tube longitudinal axis (white dotted line).

with those expected for a nanotube composed of the corresponding octapeptide rings (SI Figure S4).[16]

Sonication of purified SWCNTs in water in the presence of **CP-1**, followed by centrifugation, afforded stable aqueous dispersions of what, following deposition on holey grids, appeared in transmission electron microscopy (TEM) images as individual CNTs (SI Figure S2). These CNTs were generally associated for at least part of their length with a layer of another material that was sensitive to the electron beam even at low temperatures (Figure 1d, SI S3). The fragility of this apparent layer is consistent with a supramolecular polymer behavior under stress.[25] Sonication and centrifugation of 0.4 mg of carbon nanotubes in 1 mL aqueous solution (200 μM **CP-1**) afforded a final concentration of dispersed carbon nanotubes of 0.008 mg mL^{-1} as calculated by using UV absorption (2% dispersion yield).[12i] The prepared suspensions were stable without special conditions at room temperature for more than 6 months without any observed flocculation.

In these dispersions, UV absorption by the pyrene moiety was essentially the same as before sonication and centrifugation (Figure 2a, inset), showing that the total concentration of **CP-1** was unchanged. By contrast, 90% of pyrene fluorescence emission was quenched (SI Figure S1), reflecting interaction with CNTs. To remove the excess of CP, the SWCNT/SCPN dispersions were dialyzed. During the first 12 h, fluorescence monitoring showed a relative increase and accompanying 8 nm blue shift of the 470 nm emission band (Figure 2a), an unambiguous indication of the formation of a charge-transfer excited state complex between pyrene and CNT.[20,23] FTIR spectroscopy of the same dialyzed mixture showed the characteristic vibronic bands of the antiparallel type interaction of SCPNs (amide A, I and II) that confirms that CPs upon interaction with CNTs interact with each other to form the twin nanotubes (Figure 2b).

Following deposition of dialyzed SWCNT/SCPN dispersions on mica and copious washing of the surface with Milli-Q water, AFM topographic imaging showed tubular structures lying horizontally on the substrate with heights that varied from one tube segment to another (4 to 6 nm average, SI Figures S5, S9). In these images, it was possible to identify individual SWCNTs whose diameter increased from 1 to 4 nm (Figure 1e−f, 2c,d). The 4 nm height was consistent with a twin nanotube formed by an SWCNT and an SCPN, whereas the higher 6 nm heights might correspond to a sandwich of one

dx.doi.org/10.1021/ja410901r | J. Am. Chem. Soc. 2014, 136, 2484−2491

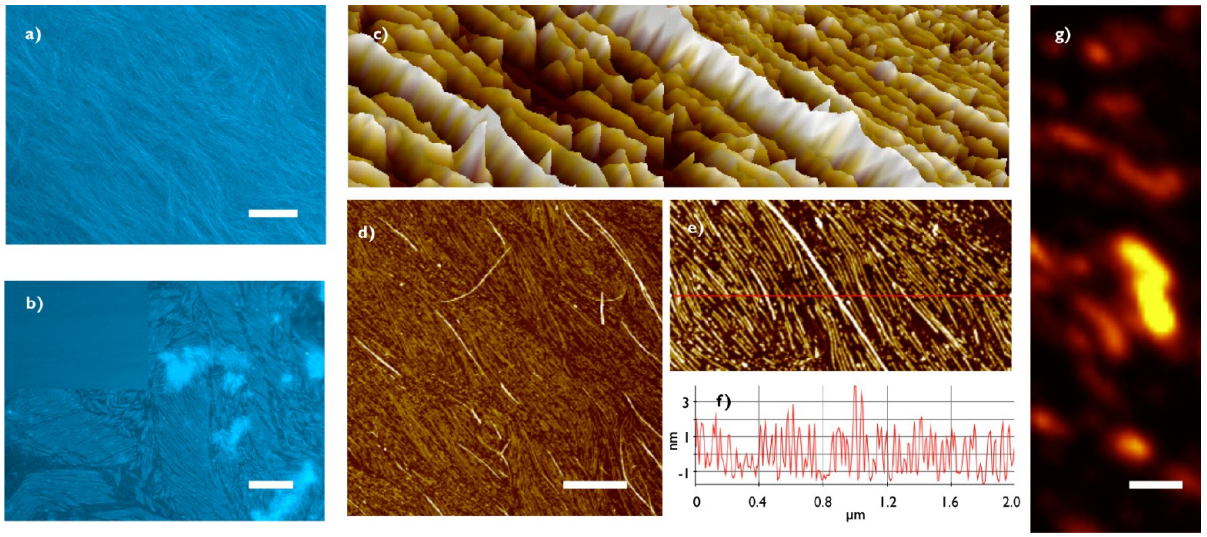

Figure 4. Ordered nanotube arrays. (a) Representative epifluorescence image of SCPNs deposited on a standard glass microscopy slide from a 500 μM solution of **CP-1** in 1:1 H_2O/CH_3CN, pH ≈ 2.5 (scale bar 10 μm). (b) As for (a), but with deposition from a 100 μM solution of pH ≈ 6−7 (scale bar 20 μm). The inset shows the almost fluorescence quenched image obtained in the presence of CNTs. (c) AFM 3D topographic image of aligned SWCNT/SCPN hybrids. (d) AFM topographic image of aligned SWCNT/SCPN hybrids (scale bar 2 μm). (e) Detail of (d). (f) Height profile along the transect shown as a red line in (e). (g) CNT Raman G band map of an array of SWCNT/SCPN hybrids on mica (scale bar 1 μm).

CNT between two peptide nanotubes (Figure 2c,e). The 3D topography images of these dispersions showed uniform and homogeneous tubular ensembles that matched well with the 3D profiles obtained from pure CP nanotubes (Figure 2d, SI S8). However, control experiments with a simpler cationic pyrene analogue (**Pyr-1**, SI Scheme S1) clearly showed uncontrolled aggregation (SI Figure S6). The importance of the **CP-1** arginine for adhesion of the SWCNT/SCPN hybrids to mica is highlighted by consideration of images obtained following deposition of CNTs solubilized with the anionic surfactant SDS, which, under the same conditions, showed only a small number of isolated nanotubes together with separate SDS aggregates (SI Figure S7).

AFM measurements in HybriD mode were also employed to acquire insights about the twin-tubes dispersions. In this measuring mode, the tip−sample distance is modulated to the quasi-harmonic law and in each oscillatory cycle the tip−sample interactions change from noncontact to contact regime. The real-time recordings of cantilever deflection and current going through the conductive AFM tip are then used to acquire local topographic, mechanical, and conductivity properties simultaneously (see SI Figure S17). The results of topography, conductivity and elasticity mapping of a 6 h dialyzed dispersion of SWCNT/SCPN is depicted in Figure 3. The topographic images in Figure 3a showed the previously discussed average diameter distributions matching single and hybrid CNTs and, interestingly, the corresponding current map (Figure 3b) showed reductions in the conductivity up to zero level in most of the high height segments. This lack of electrical conduction for the hybrid segments correlates quite well with the intrinsic higher resistivity of the peptidic tubes. The elasticity picture obtained from the real-time processing of cantilever deflection (Figure 3c) confirmed that many of the high-height isolating tubes corresponded to a softer material (blue segments). In Figure 3d, we additionally illustrate the precise values of the profiles along a drawn line that tracks the longitudinal axis of one of this hybrid tubes (Figure 3a, dotted square). The topographic profile shows a single wall carbon nanotube which diameter (~1.5 nm) increases up discontinuously to ~3.5 nm. This recurrent profile is assigned to a single CNT bound to a peptide nanotube for part of its length. In the first segment (SWCNT), the conductivity between the AFM tip and sample remains constant at around 3 nA; however, when the tube diameter grows up, the current intensity drops to levels not distinguishable from the background. This type of picture, resembling an isolated molecular nanocable, was also achievable by spreading resistance AFM in contact mode (SI Figure S10). The stiffness profile emphasizes the differences between similar dimensional materials with very different elastic modulus, being softer segments coincident with the high diameter and reduced conductivity sections and also consistent with the higher elasticity of a supramolecular nanotube attached to a carbon nanotube.

To further characterize the coupled nanotubes, we have compared the Raman spectra of the lyophilized supernatant of SWCNT/**CP-1** dispersions with those of as prepared CNTs (before mixing with **CP-1**) and with the precipitated CNTs obtained after the centrifugation step (SI Figures S11 and S12). The minimal intensity of the D band in all these spectra confirmed that the structural integrity of the CNTs was well preserved during sonication and centrifugation. That **CP-1** was also unaltered by these procedures was likewise confirmed by HPLC analysis.

Alignment. Given that for many proposed applications of nanotubes it is desirable to align them with their axes all in the same direction,[11,26−28] we investigated whether SWCNT/SCPN hybrids were amenable to align over different surfaces. Rather than embark on the micropatterning of the substrate to ensure strict alignment, we looked for the formation of ordered domains of nanotubes upon evaporation of unpinned droplets of nanotube dispersion. To identify suitable conditions for ordered array deposition, we first worked with uncoupled SCPNs, which unlike SWCNT/SCPN hybrids (Figure 4a,b) had the advantage of being observable by epifluorescence microscopy. Slow evaporation of 0.1−1.0 mM **CP-1** solutions on standard microscopy slides consistently afforded large arrays

dx.doi.org/10.1021/ja410901r | J. Am. Chem. Soc. 2014, 136, 2484−2491

of essentially parallel nanotubes (Figures 4a,b and SI S14). The arrays were most dense when evaporation was performed at low temperature (5 °C) from relatively concentrated solutions in 1:1 water/acetonitrile. In these fluorescence images, we could confirm the topological defects typical of nematic liquid crystal arrays (SI Figures S13 and S14).[27,28] The mediation of a liquid-crystalline phase is supported both by these defects and by the dependence on concentration and evaporation rate. No deposition of fibers occurred at pH 8−9, in consonance with the importance of ionic interactions in the self-assembly and deposition of SCPNs.[29] Unfortunately, the emission quenching in the SWCNT/SCPN dispersions inhibited the characterization of the aligned hybrids by epifluorescence (Figure 4b inset). For examination by AFM techniques, the deposition of nanotube arrays from undialysed SWCNT/**CP-1** mixtures was investigated using mica as substrate. Alignment was slightly more difficult to reproduce in mica than on glass, probably due to the strong interaction of SCPNs with the anionic mica surface, but was unmistakable when achieved (Figure 4c−g). 3D topographic images showed the uniform profiles observed previously (cf., Figures 2d and 4c), while the height distribution between 1 and 4 nm suggested the presence of uncoupled CNTs and SCPNs as well as hybrids (Figure 4f). That the deposited arrays did indeed contain CNTs as well as SCPNs was unambiguously confirmed by confocal Raman spectroscopy under 532 nm laser illumination. The characteristic shape of the CNT Raman spectrum was easily identified at multiple sites in a 10 × 10 μm^2 field, and a map of G band intensity showed uniformly oriented linear sources (Figure 4g).

To acquire further microscopic insights in the aligned tubular arrays we also measured the previously mentioned Hybrid Mode microscopy images in micas in which the oriented tubular networks were formed after slow evaporation of the solvent. We could discriminate the different nature of carbon, peptide, and hybrid tubes (higher in topography) by the intrinsic higher elasticity of the supramolecular arrangements (SI Figure S16).

Selectivity for Semiconducting SWCNTs. The Raman spectra of pure CNT preparations that were obtained under illumination at 785 nm showed intense radial breathing modes (RBM) at 140−180 cm^{-1} (SI Figure S12). Since the CNTs used in this study had diameters of 1.3−1.8 nm,[30] as measured by TEM and/or resonant Raman scattering,[31] these RBM peaks derived from metallic CNTs.[31−33] The RBM lower intensity in the spectra of SWCNT/SCPN preparations (SI Figure S12) therefore suggests that **CP-1** attached preferentially to semiconducting CNTs. This hypothesis is further supported by the Lorentzian shape of the G band (SI Figure S12),[31] and by comparison of the near-infrared absorption spectra of dispersions of SWCNTs in **CP-1** and SDS solutions, in which the spectra of the SWCNT/SCPN dispersions showed greater absorbance at the semiconducting van Hove optical transitions S33 and S22 (Figure 5).

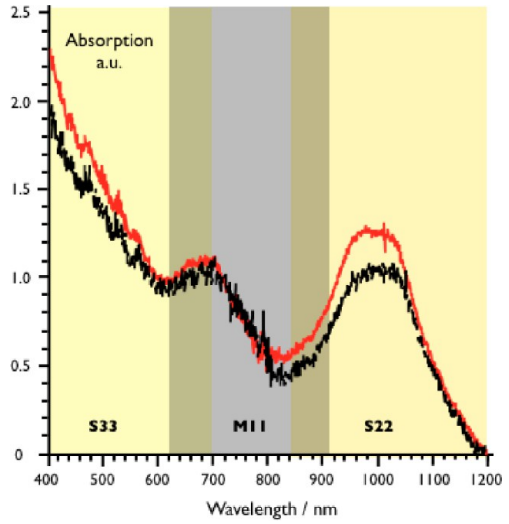

Figure 5. Compiled NIR absorbance spectra of SWCNT/SCPN and SWCNT/SDS dispersions. Each spectrum shown is the average of four separate independently prepared dispersions. The metallic first-order van Hove optical transition (M11) is shown on a gray ground, the semiconducting second- and third-order optical transitions (S22, S33) on a yellow ground. The red line corresponds to **CP-1** dispersions and the black line to SDS dispersions.

DISCUSSION

The objective of this study was to create and investigate hybrid double nanotube architectures resulting from the coupling of two of the most important nanotubular motifs: the SCPNs and the single-walled CNTs. The methodology involved the design and synthesis of cyclic peptide monomers capable of binding noncovalently to CNTs and to each other (to form the SCPN), and of maintaining the SWCNT/SCPN hybrid in aqueous solution. To exemplify the incorporation of additional capabilities, we also required the cyclic peptides to include a residue suitable for binding to an anionic solid surface. To fulfill these aims we used CPs in which D-α,γ-Acp alternated with hydrophilic L-α-amino acids, including an arginine orthogonal to a pyrene-bearing lysine.

Stable dispersion of individual CNTs in solutions of these CPs was achieved by sonication followed by centrifugation. Evidence for the intended pyrene−CNT interaction emerged when progressive removal of free CP by dialysis suppressed the 470 nm fluorescence band due to pyrene−pyrene excimers, thereby unmasking a band at shorter wavelengths attributable to a pyrene−CNT exciplex. At the same time, the ATR-FTIR spectra of samples of dialyzed CNTs dispersions showed bands typical of hydrogen bonding between antiparallel flat CPs, thus confirming the formation of SCPNs. TEM images (Figures 1d and SI S3) showed individualized CNTs associated for at least part of their length with a "coating", the lability of which was coherent with its consisting of a supramolecular polymer such as a SCPN. Topographic AFM images of the same dispersions on mica revealed individual CNTs with heights that varied from 1 to 4−6 nm along their length (Figures 1e, 2c, and SI S5), in consonance with the attachment of SWCNT/SCPN hybrids to the anionic mica surface via the cationic CP residues. The higher resistivity and softness of this hybridized segments also supports the presence of an isolating peptidic nanotubular coverage along the CNTs. The integrity of the CNT nanotubes in SWCNT/SCPN hybrids was supported by Raman spectroscopy.

The slow evaporation of **CP-1** solutions on glass resulted in the deposition of well-aligned arrays of SCPNs. The crucial importance of evaporation rate and cyclic peptide concentration in the orientation of our SCPNs suggested a convective flow oriented self-assembly of the peptide nanotubes at the liquid−solid−air interphase.[27,28] A liquid-crystalline mechanism is reinforced in view of the appearance of topological defects typical of nematic liquid crystals (SI Figure S14). Dispersions of SWCNT/SCPN hybrids afforded similar arrays on mica.

dx.doi.org/10.1021/ja410901r | J. Am. Chem. Soc. 2014, 136, 2484−2491

The preference for semiconducting carbon nanotubes in the twin hybrids is not clear, although based on the recently described selectivity of SWCN sorting by aromatic (fluorenyl) polymers,[34] we believe that the stabilization of a particular hybrid is derived from the relative orientation, distance, and backbone rigidity of the SCPN. In our dual supramolecular hybrids, the cyclic peptide scaffold and the aromatic pyrene moiety are responsible of the self-assembly (by hydrogen bonding) and of the carbon nanotube interaction ($\pi-\pi$), respectively. Thus, it is likely that peptide nanotube structure preorganize pyrene moieties to stabilize or destabilize certain types of hybrids in solution depending on diameter, chirality, and metallic character of the carbon nanotube. The finding that in the Raman spectra of SWCNT/SCPN hybrids the metallic RBM bands were much less intense than in those of pure CNT preparations, and comparison of the NIR spectra of **CP-1**- and SDS-dispersed CNTs (Figure 4), suggest that **CP-1** binds preferentially to semiconducting CNTs. The observed self-sorting toward semiconducting CNTs hybrids may derive from the regular spacing of CPs in the SCPNs being such as to favor the positioning of their pyrenes so as to maximize $\pi-\pi$ interactions with the CNT that would depend on diameter, rolling vector, and electronic properties of the CNT.[34]

CONCLUSIONS

To sum up, we report the first preparation of double nanometric tubes consisting of coupled single-walled carbon nanotubes and cyclic peptide nanotubes. These hybrid structures are created as stable dispersions and their deposition in orderly arrays is effortlessly achieved. The straightforward synthesis of the cyclic peptide scaffold, with complete control of diameter and functionalization, turns this methodology into an advantageous protocol for the alignment of target molecules at a controlled distance along the carbon nanotube longitudinal axis. The coupling of peptide and carbon nanotubes described here also offers a promising concept for the fabrication of short-circuits free conducting nanowires. The finding that those prepared in the present study were more likely to contain semiconducting than metallic CNTs invites the identification of CPs that optimize this selectivity and so facilitate SCPN-mediated separation of metallic and semiconducting CNTs after suitable workup. It is also anticipated that appropriate functionalization of CPs may allow the controlled SCPN-mediated manipulation of SWCNTs in a variety of environments (e.g., on patterned surfaces), so enhancing their technological value. In the longer term, control of the behavior of SCPNs via attached CNTs is another possibility. Our efforts in all these directions will be reported in due course.

Full experimental details of synthesis and characterization (NMR, HPLC, MS, etc.), and further details of VisUV, NIR, fluorescence, and Raman and AFM characterization, can be found online in the SI.

ASSOCIATED CONTENT

Supporting Information

Supplementary figures and details on experimental procedures, including: Materials and methods; abbreviations; synthesis of artificial amino acids and Pyr-1; synthesis of CP-1; preparation of SWCNT/SCPN aqueous dispersion; fluorescence and ART-FTIR spectroscop; transmission electron microscopy (TEM); atomic force microscopy (AFM); epifluorescence; standard Raman spectroscopy; and confocal Raman mapping. This material is available free of charge via the Internet at http://pubs.acs.org.

AUTHOR INFORMATION

Corresponding Author

javier.montenegro@usc.es; juanr.granja@usc.es

Present Address

Singular research center in chemical biology and molecular materials, (CIQUS), Organic Chemistry Department, University of Santiago de Compostela (USC), Santiago de Compostela, Spain.

Notes

The authors declare no competing financial interest.

ACKNOWLEDGMENTS

This work was supported by the Spanish Ministry of Economy and Competitivity (MEC) and the ERDF [CTQ2010-15725, and Consolider Ingenio 2010 (CSD2007-00006)], by the Xunta de Galicia (GPC2013-039), and by the European project Magnifyco (NMP4-SL-2009-228622). J.M. received a Juan de la Cierva contract from the MEC. We thank Mercedes Rivas and Raquel Antón from University of Santiago de Compostela (CACTUS) and Benito Rodríguez González University of Vigo (CACTI) for assistance with electron and fluorescence microscope. We also thank Prof. Francisco Rivadulla University of Santiago de Compostela University of Santiago de Compostela (CIQUS) for assistance with the gold mask sputtering.

REFERENCES

(1) Bong, D.; Clark, T.; Granja, J.; Ghadiri, M. *Angew. Chem., Int. Ed.* **2001**, *40*, 988−1011.

(2) Saito, M. S.; Dresselhaus, R.; Dresselhaus, G. M. *Physical Properties of Carbon Nanotubes*; Imperial College Press: London, 1998.

(3) (a) Omachi, H.; Nakayama, T.; Takahashi, E.; Segawa, Y.; Itami, K. *Nat. Chem.* **2013**, *5*, 572−576. (b) Yum, K.; Ahn, J.-H.; McNicholas, T. P.; Barone, P. W.; Mu, B.; Kim, J.-H.; Jain, R. M.; Strano, M. S. *ACS Nano* **2012**, *6*, 819−830. (c) Dieckmann, G. R.; Dalton, A. B.; Johnson, P. A.; Razal, J.; Chen, J.; Giordano, G. M.; Muñoz, E.; Musselman, I. H.; Baughman, R. H.; Draper, R. K. *J. Am. Chem. Soc.* **2003**, *125*, 1770−1777. (d) Williams, K. A.; Veenhuizen, P.; de la Torre, B. G.; Eritja, R.; Dekker, C. *Nature* **2002**, *420*, 761.

(4) Ajayan, P. M. *Chem. Rev.* **1999**, *99*, 1787−1800.

(5) Strano, M. S.; Boghossian, A. A.; Kim, W.-J.; Barone, P. W.; Jeng, E. S.; Heller, D. A.; Nair, N.; Jin, H.; Sharma, R.; Lee, C. Y. *MRS Bull.* **2009**, *34*, 950−961.

(6) (a) Singh, P.; Campidelli, S.; Giordani, S.; Bonifazi, D.; Bianco, A.; Prato, M. *Chem. Soc. Rev.* **2009**, *38*, 2214−2230. (b) Tasis, D.; Tagmatarchis, N.; Bianco, A.; Prato, M. *Chem. Rev.* **2006**, *106*, 1105−1136.

(7) (a) Maeda, Y.; Higo, J.; Amagai, Y.; Matsui, J.; Ohkubo, K.; Yoshigoe, Y.; Hashimoto, M.; Eguchi, K.; Yamada, M.; Hasegawa, T.; Sato, Y.; Zhou, J.; Lu, J.; Miyashita, T.; Fukuzumi, S.; Murakami, T.; Tohji, K.; Nagase, S.; Akasaka, T. *J. Am. Chem. Soc.* **2013**, *135*, 6356−6362. (b) Mu, B.; McNicholas, T. P.; Zhang, J.; Hilmer, A. J.; Jin, Z.; Reuel, N. F.; Kim, J.-H.; Yum, K.; Strano, M. S. *J. Am. Chem. Soc.* **2012**, *134*, 17620−17627. (c) Strano, M. S. *J. Am. Chem. Soc.* **2003**, *125*, 16148−16153. (d) Georgakilas, V.; Kordatos, K.; Prato, M.; Guldi, D. M.; Holzinger, M.; Hirsch, A. *J. Am. Chem. Soc.* **2002**, *124*, 760−761.

(8) Britz, D. A.; Khlobystov, A. N. *Chem. Soc. Rev.* **2006**, *35*, 637−659.

(9) Ortiz-Acevedo, A.; Xie, H.; Zorbas, V.; Sampson, W. M.; Dalton, A. B.; Baughman, R. H.; Draper, R. K.; Musselman, I. H.; Dieckmann, G. R. *J. Am. Chem. Soc.* **2005**, *127*, 9512−9517.

(10) Ehli, C.; Oelsner, C.; Guldi, D. M.; Mateo-Alonso, A.; Prato, M.; Schmidt, C.; Backes, C.; Hauke, F.; Hirsch, A. *Nat. Chem.* **2009**, *1*, 243−249.
(11) (a) Jin, S. H.; Dunham, S. N.; Song, J.; Xie, X.; Kim, J.-H.; Lu, C.; Islam, A.; Du, F.; Kim, J.; Felts, J.; Li, Y.; Xiong, F.; Wahab, M. A.; Menon, M.; Cho, E.; Grosse, K. L.; Lee, D. J.; Chung, H. U.; Pop, E.; Alam, M. A.; King, W. P.; Huang, Y.; Rogers, J. A. *Nat. Nanotech.* **2013**, *8*, 347−355. (b) Lemieux, M. C.; Roberts, M.; Barman, S.; Jin, Y. W.; Kim, J. M.; Bao, Z. *Science* **2008**, *321*, 101−104. (c) Wang, F.; Gu, H.; Swager, T. M. *J. Am. Chem. Soc.* **2008**, *130*, 5392−5393. (d) Kang, S. J.; Kocabas, C.; Ozel, T.; Shim, M.; Pimparkar, N.; Alam, M. A.; Rotkin, S. V.; Rogers, J. A. *Nat. Nanotech.* **2007**, *2*, 230−236. (e) Wang, Y.; Maspoch, D.; Zou, S.; Schatz, G. C.; Smalley, R. E.; Mirkin, C. A. *Proc. Natl. Acad. Sci., U. S. A.* **2006**, *103*, 2026−2031.
(12) (a) Liu, G.; Wang, F.; Chaunchaiyakul, S.; Saito, Y.; Bauri, A. K.; Kimura, T.; Kuwahara, Y.; Komatsu, N. *J. Am. Chem. Soc.* **2013**, *135*, 4805−4814. (b) Tanaka, T.; Urabe, Y.; Nishide, D.; Kataura, H. *J. Am. Chem. Soc.* **2011**, *133*, 17610−17613. (c) Carvalho, E. J. F.; dos Santos, M. C. *ACS Nano* **2010**, *4*, 765−770. (d) Tanaka, T.; Jin, H.; Miyata, Y.; Fujii, S.; Suga, H.; Naitoh, Y.; Minari, T.; Miyadera, T.; Tsukagoshi, K.; Kataura, H. *Nano Lett.* **2009**, *9*, 1497−1500. (e) Arnold, M. S.; Green, A. A.; Hulvat, J. F.; Stupp, S. I.; Hersam, M. C. *Nat. Nanotech.* **2006**, *1*, 60−65. (f) Maeda, Y.; Kimura, S.-I.; Kanda, M.; Hirashima, Y.; Hasegawa, T.; Wakahara, T.; Lian, Y.; Nakahodo, T.; Tsuchiya, T.; Akasaka, T.; Lu, J.; Zhang, X.; Yu, Y.; Nagase, S.; Kazaoui, S.; Minami, N.; Shimizu, T.; Tokumoto, H.; Saito, R. *J. Am. Chem. Soc.* **2005**, *127*, 10287−10290. (g) Li, H.; Zhou, B.; Lin, Y.; Gu, L.; Wang, W.; Fernando, K. A. S.; Kumar, S.; Allard, L. F.; Sun, Y.-P. *J. Am. Chem. Soc.* **2004**, *126*, 1014−1015. (h) Chattopadhyay, D.; Galeska, I.; Papadimitrakopoulos, F. *J. Am. Chem. Soc.* **2003**, *125*, 3370−3375. (i) Giordani, S.; Bergin, S. D.; Nicolosi, V.; Lebedkin, S.; Kappes, M. M.; Blau, W. J.; Coleman, J. N. *J. Phys. Chem. B* **2006**, *110*, 15708−15718.
(13) (a) Zheng, M.; Jagota, A.; Semke, E. D.; Diner, B. A.; McLean, R. S.; Lustig, S. R.; Richardson, R. E.; Tassi, N. G. *Nat. Mater.* **2003**, *2*, 338−342. (b) Xin, H.; Woolley, A. T. *J. Am. Chem. Soc.* **2003**, *125*, 8710−8711.
(14) Tu, X.; Manohar, S.; Jagota, A.; Zheng, M. *Nature* **2009**, *460*, 250−253.
(15) (a) Montenegro, J.; Ghadiri, M. R.; Granja, J. R. *Acc. Chem. Res.* **2013**, *46*, 2955−2965. (b) Fernandez-Lopez, S.; Kim, H.-S.; Choi, E. C.; Delgado, M.; Granja, J. R.; Khasanov, A.; Kraehenbuehl, K.; Long, G.; Weinberger, D. A.; Ghadiri, K. M. W. M. R. *Nature* **2001**, *412*, 452−456. (c) Ghadiri, M. R.; Granja, J. R.; Buehler, L. K. *Nature* **1994**, *369*, 301−304.
(16) (a) Garcia-Fandiño, R.; Amorin, M.; Castedo, L.; Granja, J. R. *Chem. Sci.* **2012**, *3*, 3280−3285. (b) Reiriz, C.; Brea, R. J.; Arranz, R.; Carrascosa, J. L.; Garibotti, A.; Manning, B.; Valpuesta, J. M.; Eritja, R.; Castedo, L.; Granja, J. R. *J. Am. Chem. Soc.* **2009**, *131*, 11335−11337.
(17) Brea, R. J.; Reiriz, C.; Granja, J. R. *Chem. Soc. Rev.* **2010**, *39*, 1448−1456.
(18) (a) Choi, W.; Lee, C. Y.; Ham, M.-H.; Shimizu, S.; Strano, M. S. *J. Am. Chem. Soc.* **2011**, *133*, 203−205. (b) Lee, C. Y.; Choi, W.; Han, J. H.; Strano, M. S. *Science* **2010**, *329*, 1320−1324.
(19) Chen, R. J.; Zhang, Y.; Wang, D.; Dai, H. *J. Am. Chem. Soc.* **2001**, *123*, 3838−3839.
(20) Martin, R. B.; Qu, L.; Lin, Y.; Harruff, B. A.; Bunker, C. E.; Gord, J. R.; Allard, L. F.; Sun, Y.-P. *Phys. Chem. B* **2004**, *108*, 11447−11453.
(21) Tomonari, Y.; Murakami, H.; Nakashima, N. *Chem.—Eur. J.* **2006**, *12*, 4027−4034.
(22) Ehli, C.; Rahman, G. M. A.; Jux, N.; Balbinot, D.; Guldi, D. M.; Paolucci, F.; Marcaccio, M.; Paolucci, D.; Melle-Franco, M.; Zerbetto, F.; Campidelli, S.; Prato, M. *J. Am. Chem. Soc.* **2006**, *128*, 11222−11231.
(23) (a) Zhang, Y.; Yuan, S.; Zhou, W.; Xu, J.; Li, Y. *J. Nanosci. Nanotech.* **2007**, *7*, 2366−2375. (b) Poenitzsch, V. Z.; Winters, D. C.; Xie, H.; Dieckmann, G. R.; Dalton, A. B.; Musselman, I. H. *J. Am. Chem. Soc.* **2007**, *129*, 14724−14732.
(24) Kim, H. S.; Hartgerink, J. D.; Ghadiri, M. R. *J. Am. Chem. Soc.* **1998**, *120*, 4417−4424.
(25) Rosenthal-Aizman, K.; Svensson, G.; Undén, A. *J. Am. Chem. Soc.* **2004**, *126*, 3372−3373.
(26) (a) Sharma, R.; Strano, M. S. *Adv. Mater.* **2009**, *21*, 60−65. (b) Sharma, R.; Lee, C. Y.; Choi, J. H.; Chen, K.; Strano, M. S. *Nano Lett.* **2007**, *7*, 2693−2700.
(27) Ko, H.; Tsukruk, V. V. *Nano Lett.* **2006**, *6*, 1443−1448.
(28) Zhang, S.; Li, Q.; Kinloch, I. A.; Windle, A. H. *Langmuir* **2010**, *26*, 2107−2112.
(29) The same pH dependence for the SCPNs assembly was corroborated by AFM.
(30) Kim, D. S.; Nepal, D.; Geckeler, K. E. *Small* **2005**, *1*, 1117−1124.
(31) (a) Dresselhaus, M. S.; Dresselhaus, G.; Jorio, A.; Souza Filho, A. G.; Pimenta, M. A.; Saito, R. *Acc. Chem. Res.* **2002**, *35*, 1070−1078. (b) Jorio, A.; Saito, R.; Hafner, J.; Lieber, C.; Hunter, M.; McClure, T.; Dresselhaus, G.; Dresselhaus, M. *Phys. Rev. Lett.* **2001**, *86*, 1118−1121.
(32) Kataura, H.; Kumazawa, Y.; Maniwa, Y.; Umezu, I.; Suzuki, S.; Ohtsuka, Y.; Achiba, Y. *Synth. Met.* **1999**, *103*, 2555−2558.
(33) Weisman, R. B.; Bachilo, S. M. *Nano Lett.* **2003**, *3*, 1235−1238.
(34) (a) Hwang, J.-Y.; Nish, A.; Doig, J.; Douven, S.; Chen, C.-W.; Chen, L.-C.; Nicholas, R. J. *J. Am. Chem. Soc.* **2008**, *130*, 3543−3553. (b) Nish, A.; Hwang, J.-Y.; Doig, J.; Nicholas, R. J. *Nat. Nanotech.* **2007**, *2*, 640−646.